

Real time mitochondrial dimension measurements

Joseph M. Leichner, Evgene Konyukhov, David Kamoun, Yael Yaniv*

Biomedical Engineering Faculty, Technion-IIT, Haifa 32000, Israel

*Corresponding author: Yael Yaniv, Email: yaely@bm.technion.ac.il

Competing interests: The authors have declared that no competing interests exist.

Abbreviations used: FFT, fast Fourier transformation; IV, intravenous; ROI, region of interest; ROS, reactive oxygen species; SL, sarcomere length; SN, serial number; 2D, two dimension

Received May 3, 2018; Revision received July 31, 2018; Accepted August 8, 2018; Published March 27, 2019

ABSTRACT

Mitochondrial volume is correlated with cell function and internal cell processes. Changes in mitochondrial volume were associated with advanced states of cardiac disease. Thus, measurements of mitochondrial dimension deformations are important to the understanding of cell function and its deterioration. Existing methods either allow measurements of the volume of isolated mitochondria, which are an inferior model to that of isolated cells, or they allow short time measurements that are toxic to the cells. Recent studies have discovered that mitochondrial deformation along a given cell axis can be measured by using the Fourier transformation on the variation in transmitted light intensity induced by the periodic lattice of myofilaments alternating with mitochondrial rows. However, this method was used only offline and in a line scan mode, making it impossible to measure both axes. We designed an open source program in LabVIEW to take advantage of the transmitted light diffraction technique and quantify mitochondrial two dimension (2D) deformation in cardiomyocytes, *in situ* in real time for long periods (more than several seconds). We validated the program on synthetic and on experimental images from rabbit and rat ventricular myocytes. The program can analyze offline and real time simultaneous 2D mitochondrial deformation dynamics as well as also sarcomere length dynamics. Moreover, the program can accurately analyze images acquired from different cameras. Quantification of mitochondrial 2D deformations is a powerful tool for exploring cell biophysics and bioenergetics mechanisms and will lay the foundation for a future clinical tool for quantifying mitochondrial volume changes associated with different cardiac diseases.

Keywords: energetics, mitochondrial deformation, mitochondrial volume, real time, sarcomere length

INTRODUCTION

Mitochondrial volume is associated with several processes in the cell: mitochondrial volume correlates with energy production [1], reactive oxygen species (ROS) formation [2], cytochrome c release in the process of apoptosis [3], and force development by the myofibrils [4]. Thus, measurements of mitochondrial dimension can be useful for exploring how the cell maintains its function during normal and abnormal conditions and how changes in mitochondrial dimensions are associated with different cardiac diseases.

Different techniques have been suggested to measure mitochondrial dimensions. The most popular technique is light scattering [5]. However, this technique provides information only for isolated mitochondria, which are an inferior physiological model to that of isolated cells [6]. Mitochondrial potential dye can be used to image mitochondrial dimensions [7], but this technique is applicable for short imaging only; long imaging is not possible because the potential dye produces ROS in the cell. Moreover, small deformations of the mitochondria in response to

cell contraction are below the diffraction limit. Finally, while electron microscopy can image the cell with the necessary resolution [8], the cell must be fixed, and thus no functional information about the cell can be obtained.

A recent microscopy technique makes use of the tight packing of the mitochondria between the sarcomeres in the cardiac cell and the fact that there are two mitochondria per sarcomere [2]. In this technique, laser diffraction without dyes is used to measure the steady state sarcomere length (SL) and the mitochondrial dimensions *in situ*. This technique was further developed so that the SL and mitochondrial dimension dynamics can now be quantified in response to light pacing [9]. Although this technique allows mitochondrial dimension dynamics to be quantified *in situ* for the first time, the analysis can be done post-processing and only for short time recordings. Because the cells can only be analyzed off-line, the success rate is very low if the cell undergoes drug manipulation or other manipulations (*e.g.*, stretching). Moreover, if a large population of cells is scanned, off-line processing slows the process. Finally, because no public program is available to

How to cite this article: Leichner JM, Konyukhov E, Kamoun D, Yaniv Y. Real time mitochondrial dimension measurements. *J Biol Methods* 2019;6(1):e111. DOI: 10.14440/jbm.2019.262

analyze the mitochondrial dimensions, this method is not widely used.

We aim to develop a real-time open source program to analyze SL and mitochondrial dimension dynamics from cardiomyocytes isolated from different mammals. The program will also be able to carry out post-processing analysis for existing data. Finally, the program will be able to analyze real-time data from different microscope systems.

METHODS

Animal use

Animals were treated in accordance with the Technion Ethics Committee. The experiment protocols were approved by the Animal Care and Use Committee of the Technion (Ethics numbers: IL-118-10-13 and IL-050-05-15).

Rabbit ventricular cell isolation

Hearts were isolated from healthy male New Zealand White rabbits weighing 2.3–2.7 kg. Each rabbit was weighed and sedated through administration of an intramuscular injection containing ketamine (0.1 ml/kg) and xylazine (0.1 ml/kg). An intravenous (IV) cannula was inserted in the rabbit's ear for the future use of an anesthetic. The rabbit was administered 200 mg/kg sodium pentobarbital diluted with heparin through the IV cannula. The adequacy and efficiency of the anesthesia were examined by observing the loss of reflexes in the eye and foot. The procedure to isolate the ventricular cells is described in [10].

Rat ventricular cell isolation

Hearts were isolated from 2–4 month old Sprague-Dawley rats. The rats were administered 200 mg/kg sodium pentobarbital diluted with heparin injected to belly. Deep anesthesia was verified by checking

absence of reflexes on repeated foot pinch and eye touch. The procedure for isolating the ventricular cells is described in [9].

Cell imaging

Cell imaging was carried out at 36°C. Cells were imaged with an ECLIPSE TE2000S inverted microscope (Nikon) using a 60× CFI plan lens. Transmitted optics images were acquired using a C4742-80-12AG Hamamatsu camera at 0.155 pixel/μm at a rate of 25 frame/s.

Analysis program

The program was written using LabVIEW (National Instruments), because it interfaces extremely well with external devices, including cameras, allowing us to analyze the image sequences acquired by the camera in real time. The main screen of the program at start up is presented in **Figure 1**. The buttons at the top of the screen were split into sections (colored in light blue) according to function. Furthermore, in order to avoid bugs, buttons are grayed out when they should not be used.

The program has two working modes. The default mode is working online, which includes real-time analysis of data acquired *via* a live camera feed. It is also possible to work in an offline mode by loading an existing AVI file and performing the analysis on it.

Data acquisition

The first step in the online mode is to configure the camera settings by clicking on the “Configure” button and selecting the desired camera. Prior to configuration, the user should ensure that the correct camera driver software is installed on the computer. Once the camera settings are configured, the user can click the “Power On” button, which will start the acquisition process, and the live feed will be visible on the main screen. The main screen upon program startup is shown in **Figure 1**.

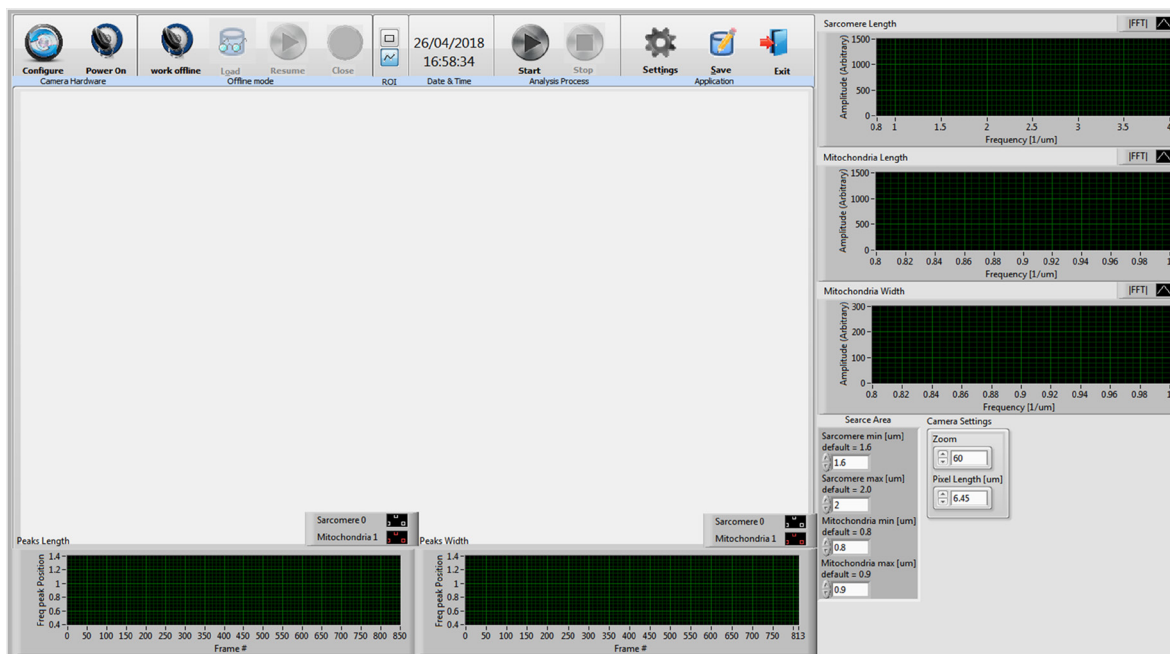


Figure 1. The main screen of the program upon startup. (1) Configure, (2) Power On/Power Off, (3) Work Offline/Stop Work Offline, (4) Load, (5) Pause/Resume, (6) Close, (7) ROI format—choose of square or line, (8) Date & time, (9) Start/Pause (process), (10) Stop (process), (11) Settings, (12) Save, (13) Exit, (14) Main screen, (15) Sarcomere and mitochondrial peak vs. frame (cell's length), (16) Mitochondrial peak vs. frame (cell's width), (17) Current sarcomere and mitochondrial peaks.

If working offline, the user must switch the program to offline mode by clicking the “Work Offline” button and then clicking the Load button, after which a select file dialog box will appear. Once the desired AVI file is selected, it will start running. The video feed will be visible on the main screen as in the “Working Online” mode. Note that when working offline, once the video has been loaded it should be immediately paused (using the “Pause” button) to select the region of interest (ROI). The user can resume the video using the “Resume” button. The “Close” button can be used at any time to stop and close the loaded AVI video. The user can return to the default offline mode at any time by clicking the “Stop Work Offline” button.

Selecting the ROI

The user can choose the ROI from the video after acquisition is activated by clicking the line icon. Because the length of the cell is significantly longer than its width, the ROI should consist of a line along the length of the cell and a number of parallel lines along its width. A single click on the video screen marks the starting point of the selected ROI. Every click on the screen will add a point to the ROI. The lines must be selected continuously, as illustrated in **Figure 2**, while the connecting diagonal lines should be ignored by the user. Note that the user must first mark the single line along the length of the cell and only then mark the lines along its width, while ensuring that the latter lines are selected roughly perpendicular to the line along the length. The user may select as many lines along the width of the cell as desired. A double click will mark the final point of the ROI. Once the ROI has been selected, the lines can be moved and edited. The user can select a new ROI at any time. The program will conduct the analysis on the current ROI.

Analysis process

The analysis contains several steps: First, the program calculates

the fast Fourier transform (FFT) of the ROI along the length of the cell, while taking the angle of the line and the zoom into account. If we define the starting point as (x_1, y_1) and the end point as (x_2, y_2) , the element length is calculated as:

$$\text{Element Length} = \frac{\left(\frac{\text{Pixel Length}}{\text{Zoom}} \right)}{\cos \left(\tan^{-1} \left(\frac{y_2 - y_1}{x_2 - x_1} \right) \right)} \quad (\text{Eqn. 1})$$

In our case the pixel size is $6.45 \mu\text{m} \times 6.45 \mu\text{m}$ and the zoom was $\times 60$. Thus:

$$\text{Element Length} = \frac{\left(\frac{6.45 \mu\text{m}}{60} \right)}{\cos \left(\tan^{-1} \left(\frac{y_2 - y_1}{x_2 - x_1} \right) \right)} \quad (\text{Eqn. 2})$$

Second, the distance in frequency units between the elements of the FFT vector (df) is calculated as:

$$df = \frac{1}{N \cdot \text{Element Length}} \quad (\text{Eqn. 3})$$

where N is defined as the number of elements of the calculated FFT vector.

Thirds, similar calculation is done for the ROI lines along the width of the cell. Because the width dimension is shorter than the length dimension, multiple lines are used for its analysis (as shown in **Fig. 2**).

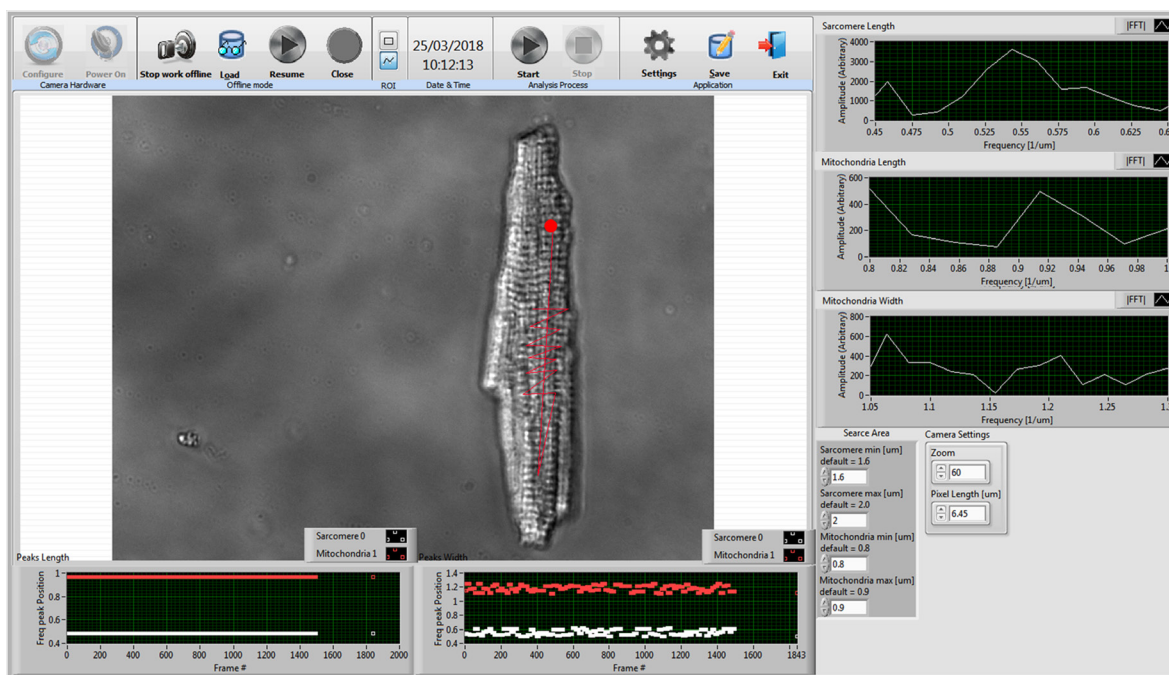


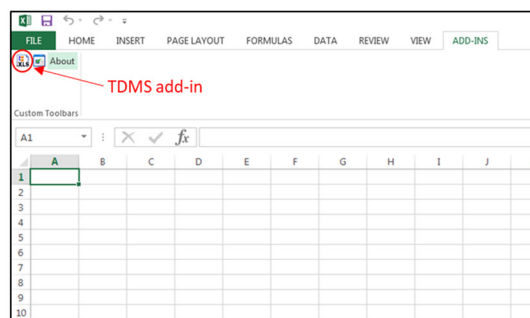
Figure 2. The main screen of the program upon uploading an image and performing analysis. The ROI selected by the user is visible on the program screen. Note that the program analyzed only the orthogonal lines and ignored the connecting lines. The red dot marks the starting point.

The program will concatenate the lines into one long line and calculate the FFT. Because the lines are close to parallel, the df of each ROI width line will be calculated separately and the average df will be used. Forth, once the program has calculated the FFTs and the corresponding dfs, it will search for the two main peaks in the FFT graphs, which correspond to sarcomere and mitochondrial length. The search will be limited to the frequency range in which these peaks are expected: 1.8 μm –2.2 μm for the sarcomere, and 0.7 μm –1.1 μm for the mitochondria. Fifth, the analysis is repeated for every frame. The per-frame change in the position of the peaks in the FFT graphs is shown in three graphs (two for the length dimension and one for the width dimension).

The “Start” button is used to start saving data from the analysis process. The saved data will produce two files: a simple AVI video file of the analyzed image sequence and a TDMS file (LabVIEW Test Data Exchange Stream, a file format for saving well-documented

measurement data using a hierarchical organization). The data from the saved TDMS file can be accessed using an Excel TDMS add-in in the “ADD-INS” tab, as shown in **Figure 3A**. The data in the Excel file will consist of two tabs, one which includes technical information about the data acquired and another that includes the data itself: the FFT, the sarcomere peaks, and the mitochondrial peaks for both length and width dimensions. An example of the data in the Excel file can be seen in **Figure 3B**. The saved files will be named using the format: ‘username_dd_mm_yy_hh_mm_ss’ and can be found in a folder called ‘SavedData’ in the program’s directory (the folder will be automatically created if it does not exist). The user can click the “Pause” button to pause the saving process and the Stop button to stop it. Once the saving process is stopped, the data files are closed and saved. Any data acquired after the analysis process is restarted will be saved in separate files.

A



B

Root Name	Title	Author	Date/Time	Groups	Description	Date_Time
Noam_2017_05_12_12_48_13	Cardiomyocytes	Noam		1		12/05/2017 12:48
Group	Channels	Description				
Data						
Data	Datatype	Unit	Length	Minimum	Maximum	Description
FFT_data_1	DT_DOUBLE		40956			Start Index
Peaks_Sarcomere_1	DT_DOUBLE		129			
Peaks_Mitochondria_1	DT_DOUBLE		129			
FFT_data_2	DT_DOUBLE		21285			
Peaks_Sarcomere_2	DT_DOUBLE		129			
Peaks_Mitochondria_2	DT_DOUBLE		129			

FFT_data_1	Peaks_Sarcomere_1	Peaks_Mitochondria_1	FFT_data_2	Peaks_Sarcomere_2	Peaks_Mitochondria_2
25400	0.482417537	1.427955009	13130	0.549023128	0.892162584
6813.862917	0.482417537	1.427955009	1204.191945	0.549023128	0.892162584
3157.302015	0.482417537	1.427955009	1982.381774	0.549023128	0.892162584
3118.532453	0.482417537	1.427955009	2168.402056	0.549023128	0.892162584
4226.02475	0.482417537	1.427955009	2400.562428	0.549023128	0.892162584
4082.487906	0.482417537	1.427955009	1314.833449	0.549023128	0.892162584
2298.151712	0.482417537	1.427955009	1203.390509	0.549023128	0.892162584
859.918174	0.482417537	1.427955009	768.9126054	0.549023128	0.892162584
2603.604583	0.482417537	1.427955009	1318.881192	0.549023128	0.892162584
2411.1298	0.482417537	1.427955009	202.7029844	0.549023128	0.892162584
4278.490996	0.482417537	1.427955009	1847.917008	0.549023128	0.892162584
3114.547148	0.482417537	1.427955009	3917.730618	0.549023128	0.892162584
7120.231777	0.482417537	1.427955009	2396.200228	0.549023128	0.892162584
3823.348539	0.482417537	1.427955009	2707.682982	0.549023128	0.892162584
3740.756825	0.482417537	1.427955009	984.2882907	0.549023128	0.892162584
3223.752872	0.482417537	1.427955009	1108.635591	0.549023128	0.892162584
4298.448774	0.482417537	1.427955009	2007.552128	0.549023128	0.892162584
791.5737696	0.482417537	1.427955009	1515.147662	0.549023128	0.892162584
2531.046693	0.482417537	1.427955009	1030.221304	0.549023128	0.892162584
1086.387612	0.482417537	1.427955009	895.6020204	0.549023128	0.892162584
1718.285535	0.482417537	1.427955009	2281.896958	0.549023128	0.892162584
1745.765579	0.482417537	1.427955009	463.1415136	0.549023128	0.892162584
2961.788906	0.548207941	1.427955009	971.492478	0.411787346	1.098046217
8129.129709	0.453472485	1.427955009	1145.970963	0.549023128	0.892162584
2567.693439	0.453472485	1.427955009	1737.39426	0.549023128	0.892162584
3297.232634	0.472789186	1.427955009	702.2155301	0.411787346	1.098046217
3508.060668	0.482417537	1.427955009	815.5166091	0.411787346	1.098046217
4912.991375	0.463120835	1.427955009	566.0281297	0.411787346	0.892162584
2223.10111	0.463120835	1.427955009	627.4196472	0.411787346	0.892162584
8127.3912373	0.346307841	1.427955009	139.5880175	0.411787346	0.892162584
1712.757628	0.482417537	1.427955009	96.9044837	0.411787346	1.098046217
1811.039998	0.453472485	1.427955009	556.4854111	0.549023128	0.892162584
4797.800513	0.453472485	1.427955009	179.7806813	0.549023128	0.892162584
1137.017284	0.472789186	1.427955009	369.8123224	0.411787346	1.098046217
2157.059979	0.472789186	1.427955009	464.370481	0.411787346	1.098046217
3790.680882	0.472789186	1.427955009	110.4001842	0.411787346	1.098046217
1314.548072	0.472789186	1.427955009	364.410386	0.411787346	1.098046217
1270.554608	0.472789186	1.427955009	555.6207023	0.411787346	1.098046217

Figure 3. Data sheet. A. Example of Excel TDMS add-in. B. Left: the tab with the technical information about the acquired data. Right: the tab with the FFT data, the sarcomere peaks, and the mitochondria peaks for both length (1) and width (2) dimensions.

The current date and time of the analysis are shown to the left of the Analysis Process buttons (“Date & Time”). The “Settings” button is used to launch the settings dialog window, in which the user can edit various settings such as Name, Place, Experiment serial number, Log file path, and any comment on the specific experiment. The “Save” button is used to generate a report in Word format based on the settings defined by the user. The report will include the current date and time, comment, place, name, serial number (SN) and an image of the cell analyzed in the current experiment. The report file will be named using the format: ‘Test_Report_SN’ and will be saved in the “Log File Path” defined by

the user in the settings dialog window. The “Exit” button can be used at any time to immediately exit the program.

RESULTS

To verify that our program can find SL and mitochondrial dimensions, we first generated a syntactic image of repetitive strips to simulate repetitive sarcomeres and mitochondria. **Figure 4** shows the program interface when the synthetic image is uploaded. After the ROI is chosen,

the first and second order FFT peaks are shown. The program accurately recognized the distance between the lines (to calculate the width length we rotated the figure).

We used rat and rabbit cardiomyocytes to test the ability of the program to measure and analyze SL and mitochondrial dimensions of such cells. In these cardiomyocytes, the sarcomeres have a lattice-like structure and thus are ideal for our analysis. **Figure 2** shows the program interface for a representative cell. After the ROI is chosen, the pattern of the SL peak and the mitochondrial length and width peaks are shown. The user can choose a ROI that has a clear pattern of strips.

Analyzing the SL and mitochondrial length and width dimensions per frame allow us to calculate them vs. time. We first demonstrated our

program on rabbit cardiomyocytes. **Figure 5A** presents the SL (derived from the frequency of the first harmonic peak of the long axis measurements), the mitochondrial length (derived from the frequency of the second harmonic peak of the same long axis), and mitochondrial width (derived from the frequency of the first harmonic peak of the short axis measurements) vs. time. On average we measured 17 cells, all of which showed clear SL and mitochondrial length and width during quiescent mode. We tested the same method on rat cardiomyocytes. **Figure 5B** presents the SL, the mitochondrial length, and the mitochondrial width vs. time. On average we measured 13 cells, all of which showed clear SL and mitochondrial length and width during quiescent mode.

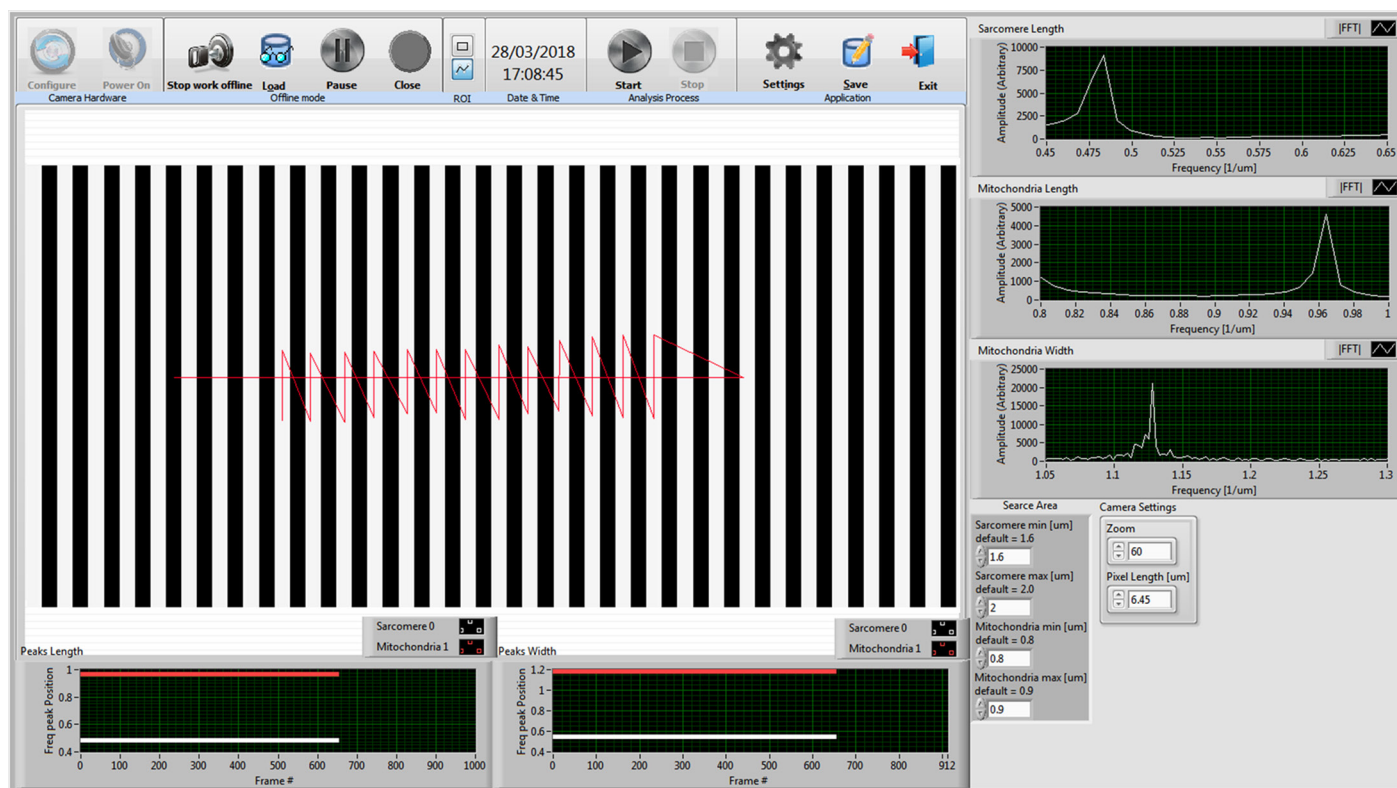


Figure 4. The main screen of the program upon uploading and analyzing the syntactic image.

Finally, we verified that our program can find SL and mitochondrial dimensions during contraction. **Figure 6** shows SL and mitochondrial contraction-relaxation cycles during steady-state 3 Hz electrical stimulation. Note that the SL shortens together with the mitochondrial length while the mitochondrial width expands, as previously documented [9]. Although we measured the steady state sarcomere and mitochondrial dimensions in 17 rabbit and 13 rat cells, we could trace only 6 steady-state sarcomere and mitochondrial contractions in each cell type. We compared our results regarding of changes in SL and mitochondrial length for rat cells that were electrically simulated at 3 Hz to results published using the same algorithm (not the same method) at a 1 Hz stimulation rate [9]. Using either electrical stimulation rate, the SL shortened together with the mitochondrial length while the mitochondrial width expanded. In response to a higher electrical stimulation rate, however, the degree of deformation of either SL or mitochondria was higher.

Upon publication of the paper, the installer of our program will be

available in .exe format at <https://bioelectric-bioenergetic-lab.net.technion.ac.il/programs/>. For instructions on how to download the program, please see our website. Please note that the program currently requires an NI Vision Run Time license.

DISCUSSION

In this work, we designed a program to analyze and measure the real time changes in sarcomere and mitochondrial dimensions *in situ*, including the possibility of conducting a later offline analysis. We have shown that the program can successfully find peaks in the FFT graphs created from a user-selected ROI in images of either rat or rabbit ventricular cells. These peaks are used to calculate the dimensional changes of the sarcomere and mitochondria. Our method is designed for the case of ventricular myocytes, where two mitochondria alternate

between a sarcomere. However, if the basic pattern of the mitochondria is different but known (*i.e.*, the location of the length peaks is known), the program can be adjusted to search around the appropriate peak (1/

basic length). Such an approach may be useful for H9c2 and HL-1 cells that undergo fusion and fission.

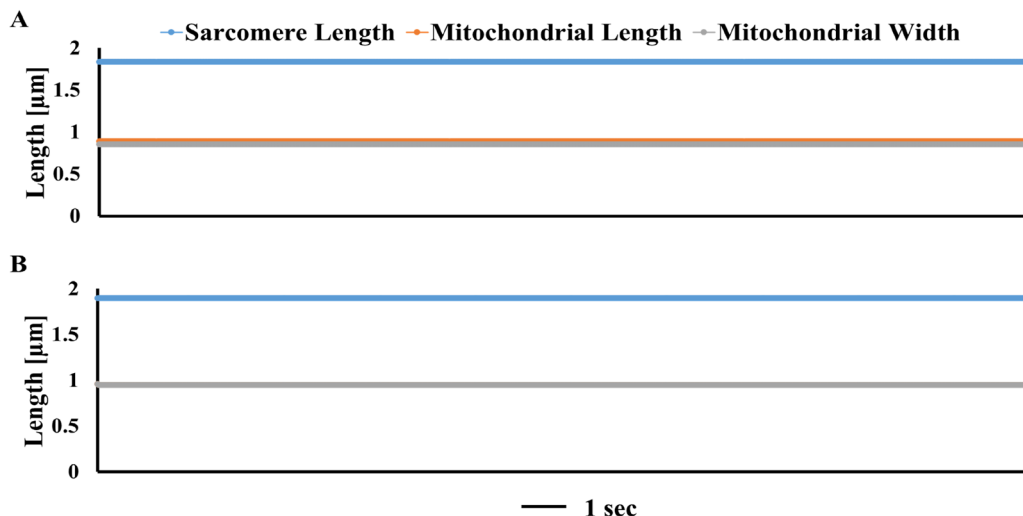


Figure 5. Representative examples of sarcomere length, mitochondrial length and mitochondrial width during rest from (A) rabbit and (B) rat cardiomyocytes.

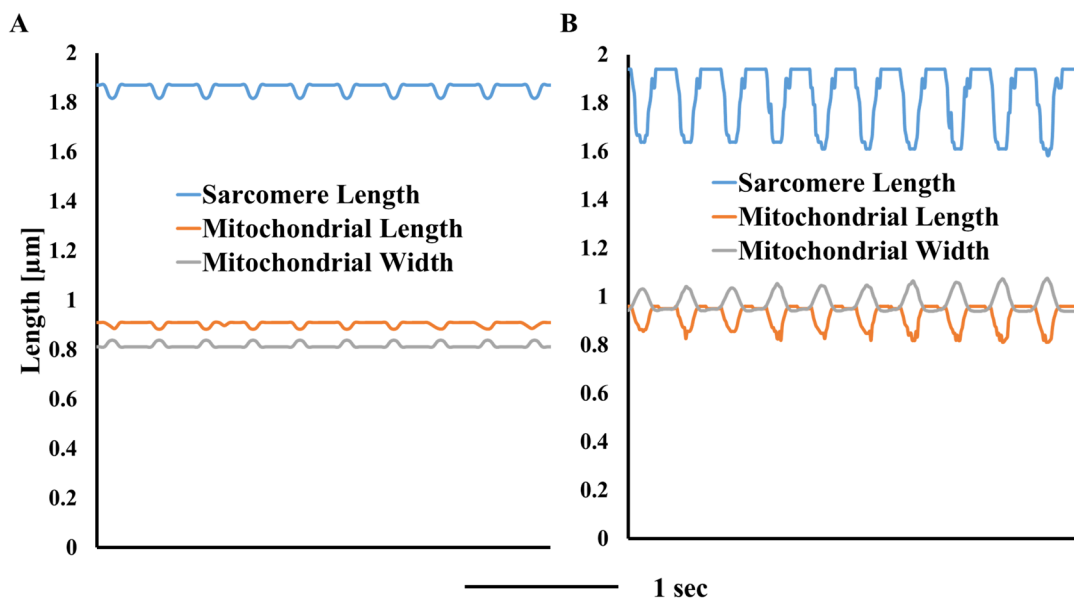


Figure 6. Representative examples of sarcomere length, mitochondrial length and mitochondrial width during contraction-relaxation cycles from (A) rabbit and (B) rat cardiomyocytes.

Mitochondrial deformations were documented here in rat and rabbit cells isolated from healthy animals. The dynamics of these deformations in response to physiological cellular alterations (*e.g.*, Ca^{2+} load of intracellular stores, cytosolic Ca^{2+} concentration, or phosphorylation state of channels) or under disease conditions are not known. Mitochondrial deformations could not be measured under these conditions due to the low success rate when using off-line analysis, especially after drug manipulation or other types of manipulation (*e.g.*, stretching the cell). We therefore aimed to develop a user-friendly program that enables

real-time calculation of the mitochondrial dimensions, thus increasing the success of *in situ* mitochondrial dimension measurements.

We chose the well-known LabVIEW environment to implement our real-time mitochondrial dimension analysis program. The program can work easily with any camera by inputting the pixel size and the zoom, thus facilitating widespread adoption of this tool.

Because no analysis program exists that can analyze mitochondrial dimensions, we generated images with syntactic bars with a known distance. The comparison between the real distance in the syntactic im-

age and the program analysis results allowed us to validate the analysis program. Note that in nature the distance between mitochondria is not necessarily homogenous. We used both rat and rabbit cardiomyocytes to show that we can find the sarcomere and mitochondrial peaks. As the analysis in **Figure 5** and **Figure 6** shows, sarcomere length and mitochondrial dimensions can be detected in real time during quiescent mode and during contractions. Our results are similar to previously obtained results [9]. We observed similar patterns of deformation for rat and rabbit cardiomyocytes.

Measurements of SL are important to quantify muscle mechanics [11], which change with cardiac diseases [12]. Thus, to understand the mechanisms that responsible for deterioration of heart function, a clear measurement of SL is needed. Mitochondrial dimensions are an unexplored area whose relationship to cardiac function is not clear. However, it is known that mitochondrial volume correlates with energy production [1], ROS formation [2], and cytochrome c release [3]. All these parameters are correlated with cell function and specifically with its deterioration. Moreover, it was shown that because the mitochondrial dynamics correspond to cytoskeletal proteins dynamics [9], tracking mitochondrial deformation can help us understand passive tension-bearing elements of the cytoskeleton. Another example is heart failure, where the sarcomere pattern is altered [13]. In myocytes isolated from the left ventricles in a tachypacing-induced heart failure canine model, the resting SL and minimal SL increases. Using our method may, in the future, reveal altered mitochondrial structure (as was documented before [14]) or even changes in their dynamics.

In summary, we presented a program for mitochondrial dimension analysis that can also analyze SL using any camera. The program runs on LabVIEW, a platform that allows real-time measurements and post-analysis processing. The program is able to measure SL and mitochondrial dimensions of cardiomyocytes and was shown here to perform successfully on rat and rabbit cardiomyocytes. We anticipate that our program will be a valuable tool for scientists studying cardiac energetics, mechanics, and the underlying mechanisms of cardiac diseases.

Author contributions

Yaniv Y conceived the project. Leichner JM and Konyukhov E designed the program. Kamoun D isolated cells. Yaniv Y and Leichner JM analyzed the data. Yaniv Y and Leichner JM wrote the paper with input from all authors. Yaniv Y supervised all aspects of the work.

Acknowledgments

The work was supported by the Israel Science Foundation, No. 882/14 (Yaniv Y). The funder had no role in study design, data collection and analysis, decision to publish, or preparation of the manuscript.

References

1. Lim KHH, Javadov SA, Das M, Clarke SJ, Suleiman M, et al. (2002) The effects of ischaemic preconditioning, diazoxide and 5-hydroxydecanoate on rat heart mitochondrial volume and respiration. *J Physiol* 545: 961-974. doi: [10.1113/jphysiol.2002.031484](https://doi.org/10.1113/jphysiol.2002.031484). PMID: 12482899
2. Juhaszova M, Zorov DB, Kim S, Pepe S, Fu Q, et al. (2004) Glycogen synthase kinase-3beta mediates convergence of protection signaling to inhibit the mitochondrial permeability transition pore. *J Clin Invest* 113: 1535-1549. doi: [10.1172/JCI19906](https://doi.org/10.1172/JCI19906). PMID: 15173880
3. Gogvadze V, Robertson JD, Enoksson M, Zhivotovsky B, Orrenius S (2004) Mitochondrial cytochrome c release may occur by volume-dependent mechanisms not involving permeability transition. *Biochem J* 378: 213-217. doi: [10.1042/BJ20031193](https://doi.org/10.1042/BJ20031193). PMID: 14629197
4. Kaasik A, Joubert F, Ventura-Clapier R, Veksler V (2004) A novel mechanism of regulation of cardiac contractility by mitochondrial functional state. *FASEB J* 18: 1219-1227. doi: [10.1096/fj.04-1508com](https://doi.org/10.1096/fj.04-1508com). PMID: 15284222
5. Tedeschi H, Harris DL (1958) Some observations on the photometric estimation of mitochondrial volume. *Biochim Biophys Acta* 28: 392-402. doi: [10.1016/0006-3002\(58\)90487-6](https://doi.org/10.1016/0006-3002(58)90487-6). PMID: 13535737
6. Yaniv Y, Juhaszova M, Nuss HB, Wang S, Zorov DB, et al. (2010) Matching ATP supply and demand in mammalian heart: in vivo, in vitro, and in silico perspectives. *Ann N Y Acad Sci* 1188: 133-142. doi: [10.1111/j.1749-6632.2009.05093.x](https://doi.org/10.1111/j.1749-6632.2009.05093.x). PMID: 20201896
7. Safulina D, Veksler V, Zharkovsky A, Kaasik A (2006) Loss of mitochondrial membrane potential is associated with increase in mitochondrial volume: physiological role in neurones. *J Cell Physiol* 206: 347-353. doi: [10.1002/jcp.20476](https://doi.org/10.1002/jcp.20476). PMID: 16110491
8. Hayashi T, Martone ME, Yu Z, Thor A, Doi M, et al. (2009) Three-dimensional electron microscopy reveals new details of membrane systems for Ca²⁺ signaling in the heart. *J Cell Sci* 122: 1005-1013. doi: [10.1242/jcs.028175](https://doi.org/10.1242/jcs.028175). PMID: 19295127
9. Yaniv Y, Juhaszova M, Wang S, Fishbein KW, Zorov DB, et al. (2011) Analysis of mitochondrial 3D-deformation in cardiomyocytes during active contraction reveals passive structural anisotropy of orthogonal short axes. *PLoS One* 6: doi: [10.1371/journal.pone.0021985](https://doi.org/10.1371/journal.pone.0021985). PMID: 21779362
10. Davoodi M, Segal S, Kirschner Peretz N, Kamoun D, Yaniv Y (2017) Semi-automated program for analysis of local Ca²⁺ spark release with application for classification of heart cell type. *Cell Calcium* 64: 83-90. doi: [10.1016/j.ceca.2017.02.003](https://doi.org/10.1016/j.ceca.2017.02.003). PMID: 28216082
11. de Tombe PP, ter Keurs HEDJ (2015) Cardiac muscle mechanics: Sarcomere length matters. *J Mol Cell Cardiol* 91: 148-150. doi: [10.1016/j.yjmcc.2015.12.006](https://doi.org/10.1016/j.yjmcc.2015.12.006). PMID: 26678623
12. Nguyen JS, Lakkis NM, Bobek J, Goswami R, Dokainish H (2010) Systolic and diastolic myocardial mechanics in patients with cardiac disease and preserved ejection fraction: impact of left ventricular filling pressure. *J Am Soc Echocardiogr* 23: 1273-1280. doi: [10.1016/j.echo.2010.09.008](https://doi.org/10.1016/j.echo.2010.09.008). PMID: 20970305
13. Gao B, Qu Y, Sutherland W, Chui RW, Hoagland K, et al. (2018) Decreased contractility and altered responses to inotropic agents in myocytes from tachypacing-induced heart failure canines. *J Pharmacol Toxicol Methods* doi: [10.1016/j.vascn.2018.06.001](https://doi.org/10.1016/j.vascn.2018.06.001). PMID: 29908289
14. Liu T, Chen L, Kim E, Tran D, Phinney BS, et al. (2014) Mitochondrial proteome remodeling in ischemic heart failure. *Life Sci* 101:27-36. doi: [10.1016/j.lfs.2014.02.004](https://doi.org/10.1016/j.lfs.2014.02.004). PMID: 24548633